$^{1,3}D^o$ resonant states in Ps^-

Y. K. Ho
Institute of Atomic and Molecular Sciences, Academia Sinica, P.O. Box 23-166, Taipei, Taiwan, Republic of China

A. K. Bhatia
Laboratory for Astronomy and Solar Physics, NASA/Goddard Space Flight Center, Greenbelt, Maryland 20771

(Received 28 March 1994)

We present a complex-coordinate rotation calculation of doubly excited $^{1,3}D^o$ resonance states in Ps^- associated with the $N=3$, $N=4$, and $N=5$ Ps thresholds. Elaborate Hylleraas-type wave functions with up to $N=1330$ terms are used. In addition to Feshbach resonances below various Ps thresholds, we have identified $^3D^o$ shape resonances with one each lying above the $N=3$ and $N=5$ Ps thresholds, respectively, as well as a $^1D^o$ shape resonance above the $N=4$ threshold. A physical interpretation of the doubly excited Ps^- is also given.

PACS number(s): 36.10.Dr, 32.80.Dz, 31.20.Di

I. INTRODUCTION

In a continuing effort to calculate resonance parameters for doubly excited states in Ps^- using the method of complex-coordinated rotation [1], we present here a calculation of $^{1,3}D^o$ doubly excited resonant states associated with the $N=3$, $N=4$, and $N=5$ Ps thresholds. Elaborate Hylleraas-type wave functions are used in the present calculation. In previous investigations, results for $^{1,3}S^e$ [2,3], $^{1,3}P^O$ [4], $^3P^e$ [5], and $^{1,3}D^e$ [6] states were reported. We have also carried out a study of P-wave shape resonances [7]. From the available theoretical results, it has been conjectured that this three-body system would behavior like an X-Y-X triatomic molecule. In order to examine such an interesting phenomenon, energy levels for states with various angular momenta and parities are needed. With the results for $^{1,3}D^O$ states reported in the present calculation, we now have resonance parameters for states with $L \le 2$. From the experimental side, Ps^- was observed in the laboratory by Mills [8]. He also measured its annihilation rate [9]. Calculations of its ground-state energy have also attracted considerable interest [10–15]. For earlier developments of investigation for this system, readers are referred to earlier reviews [16–18].

II. WAVE FUNCTIONS AND CALCULATIONS

The most general D-state wave function of odd parity of two electrons is

$$\Phi=(\sin\theta_{12})\{[(f\mp\tilde{f})\cos(\tfrac{1}{2}\theta_{12})\mathcal{D}_2^{1+}+(f\pm\tilde{f})\sin(\tfrac{1}{2}\theta_{12})\mathcal{D}_2^{1-}]$$
$$+[(5\cos\theta_{12}-1)(g\mp\tilde{g})\cos(\tfrac{1}{2}\cos\theta_{12})\mathcal{D}_2^{1+}+(5\cos\theta_{12}+1)(g\pm\tilde{g})\sin(\tfrac{1}{2}\theta_{12})\mathcal{D}_2^{1-}]\}\ , \tag{1}$$

where the $\mathcal{D}$ are the rotational harmonics, depending on the symmetric Euler angles θ,ϕ,ψ [19,20]. These functions are eigenfunctions of exchange and satisfy the following property:

$$\epsilon_{12}\mathcal{D}_1^{\kappa\pm}=\pm(-1)^{1+\kappa}\mathcal{D}_1^{\kappa\pm}\ . \tag{2}$$

The trial wave function is of the Hylleraas type and the radial functions $f=f(r_1,r_2,r_{12})$ and $g=g(r_1,r_2,r_{12})$ are given by

$$f(r_1,r_2,r_{12})=e^{-(\gamma_1 r_1+\delta_1 r_2)}r_1^2 r_2\sum_{l\ge0}\sum_{m\ge0}\sum_{n\ge0}C_{lmn}^{(1)}r_1^l r_2^m r_{12}^n\ , \tag{3}$$

$$g(r_1,r_2,r_{12})=e^{-(\gamma_2 r_1+\delta_2 r_2)}r_1^3 r_2^2\sum_{l\ge0}\sum_{m\ge0}\sum_{n\ge0}C_{lmn}^{(2)}r_1^l r_2^m r_{12}^n \tag{4}$$

with $l+m+n\le\omega$ and l, m, n, and ω being positive integers or zero. Also in Eqs. (3) and (4) we have

$$\tilde{f}=f(r_2,r_1,r_{12})\ ,\quad \tilde{g}=g(r_2,r_1,r_{12})\ . \tag{5}$$

The upper sign in Eq. (1) corresponds to the singlet states and the lower sign to the triplet states. The first term in Eq. (1) corresponds to the (pd) configuration and the second term the (df) configuration with total angular momentum $L=2$. In the present calculation we use only

the (pd) terms for practical reasons. This may slow down the convergence rate. However, as can be seen later in the text, except for one case, our results converge quite well. Up to a total of 1330 terms ($\omega=18$) are used in the present calculations.

The Hamiltonian for the ($e^-e^+e^-$) system is given by

$$H=-2\nabla_1^2-2\nabla_2^2-2\nabla_1\cdot\nabla_2-2/r_1-2/r_2+2/r_{12}=T+V\ , \tag{6}$$

where r_1 and r_2 are the coordinates of the electrons with respect to the positron and $r_{12}=|\bar{r}_1-\bar{r}_2|$. Atomic units are used in this work with energy units in rydbergs. In the complex-rotation method, the radial coordinates are rotated through an angle θ,

$$r\rightarrow r\exp(i\theta)\ , \tag{7}$$

and the Hamiltonian is transformed into

$$H=T\exp(-2i\theta)+V\exp(-i\theta)\ . \tag{8}$$

The eigenvalues are calculated by diagonalizing the expression

$$E=\langle\Phi H\Phi\rangle/\langle\Phi\Phi\rangle\ . \tag{9}$$

Since the rotated Hamiltonian is complex, complex eigenvalues are obtained. A complex resonance energy is given by

$$E_{\rm res}=E_r-i\Gamma/2\ , \tag{10}$$

with E_r the resonance energy and Γ the width.

The theoretical aspects of the complex rotation method have been discussed in previous publications [1] and will not be repeated here. Instead we only briefly describe the computational procedures. First, we use the stabilization method to obtain optimized wave functions with which complex-coordinate calculations will then be carried out. The use of the stabilization method as a first step for the method of complex-coordinate rotation has been demonstrated in a review [1]. A resonance complex eigenvalue is deduced by the stabilization condition with respect to the changes of γ_1, δ_1 [see Eq. (3)], and θ. The optimization of such parameters is usually performed with a smaller basis set, typically with $M=680$. Convergence behaviors can be examined by using different expansion lengths. Up to $M=1330$ ($\omega=18$) terms are used in the present calculations.

III. RESULTS

Table I shows the convergence behavior for the lowest $^1D^o$ state below the $N=3$ Ps threshold (threshold energy of $-0.055\,555$ Ry). The optimized parameters are obtained as $\gamma_1=\delta_1=0.32$ and $\theta=0.4$. From the results when different expansion lengths are used, we estimate the resonance parameters as $E_r=-0.060\,882\,527\,7\pm0.000\,000\,000\,2$ Ry and $\Gamma/2=0.000\,071\,953\,7\pm0.000\,000\,000\,2$ Ry. Table II shows the convergence behavior for the lowest $^1D^o$ resonance state below the $N=4$ Ps threshold (threshold energy of $-0.031\,25$ Ry) when the optimized parameters of $\gamma_1=\delta_1=0.26$ and $\theta=0.3$ are used. Using expansion lengths with up to $M=1140$ ($\omega=17$) terms, we estimate the resonance parameters as $E_r=-0.037\,098\,862\pm0.000\,000\,005$ Ry and $\Gamma/2=0.000\,023\,913\pm0.000\,000\,005$ Ry. The second $^1D^o$ resonance below the $N=4$ Ps threshold is similarly determined. The convergence behavior shown in Table III leads to resonance parameters of $E_r=-0.032\,722\,544\pm0.000\,000\,010$ Ry and $\Gamma/2=0.000\,013\,047\pm0.000\,000\,010$ Ry. In addition to the Feshbach resonances lying below the $N=4$ threshold, we have also identified a stabilized complex eigenvalue lying above the threshold. The results are shown in Table IV when the optimized values of $\gamma_1=\delta_1=0.26$ and $\theta=0.55$ are used. The relatively large value for θ is a common finding in calculations of shape resonances. It enables the cuts to be rotated farther away from the real axis. As such, the complex eigenvalues representing the cuts would not be confused with those representing shape resonances. Because of such a large θ value, the resonance wave function (after the complex transformation) would have strong oscillatory behavior with an overall exponential decaying character. This explains that in general a shape resonance converges slowly and that large expansion sets (with L^2 characters) are needed to obtain reasonably accurate results. From Table IV we determine the resonance parameters for the $N=4$ $^1D^o$ shape resonance as $E_r=-0.030\,20\pm0.000\,02$ Ry and $\Gamma/2=0.000\,40\pm0.000\,02$ Ry.

TABLE I. Convergence behavior for the $^1D^o(1)$ state below the $N=3$ Ps threshold ($\gamma_1=\delta_1=0.32$ and $\theta=0.4$).

ω	M	E (Ry)	$\Gamma/2$ (Ry)
13	560	$-0.060\,882\,528\,6$	$7.195\,32\times10^{-5}$
14	680	$-0.060\,882\,527\,7$	$7.195\,46\times10^{-5}$
15	816	$-0.060\,882\,527\,49$	$7.195\,358\times10^{-5}$
16	969	$-0.060\,882\,527\,64$	$7.195\,363\times10^{-5}$
17	1140	$-0.060\,882\,527\,71$	$7.195\,367\times10^{-5}$

TABLE II. Convergence behavior for the $^1D^o(1)$ resonance state below the $N=4$ Ps threshold ($\gamma_1=\delta_1=0.26$ and $\theta=0.3$).

ω	M	E (Ry)	$\Gamma/2$ (Ry)
12	455	$-0.037\,098\,839$	$2.389\,302\times10^{-5}$
13	560	$-0.037\,098\,860\,9$	$2.391\,860\times10^{-5}$
14	680	$-0.037\,098\,866\,7$	$2.391\,302\times10^{-5}$
15	816	$-0.037\,098\,861\,1$	$2.391\,142\times10^{-5}$
16	969	$-0.037\,098\,860\,6$	$2.391\,229\times10^{-5}$
17	1140	$-0.037\,098\,862\,1$	$2.391\,270\times10^{-5}$

TABLE III. Convergence behavior for the $^1D^o(2)$ resonance below the $N=4$ Ps threshold ($\gamma_1=\delta_1=0.2$ and $\theta=0.25$).

ω	M	E (Ry)	$\Gamma/2$ (Ry)
13	560	$-0.032\,723\,48$	1.351×10^{-5}
14	680	$-0.032\,723\,03$	1.370×10^{-5}
15	816	$-0.032\,722\,80$	1.304×10^{-5}
16	969	$-0.032\,722\,61$	1.303×10^{-5}
17	1140	$-0.032\,722\,541$	1.3042×10^{-5}
18	1330	$-0.032\,722\,544$	1.3047×10^{-5}

TABLE IV. Convergence behavior for the $^1D^o$ shape resonance lying above the $N=4$ Ps threshold with threshold energy of $-0.031\,25$ Ry ($\gamma_1=\delta_1=0.26$ and $\theta=0.55$).

ω	M	E (Ry)	$\Gamma/2$ (Ry)
13	560	−0.003 020 9	0.000 393 2
14	680	−0.030 211 5	0.000 397 0
15	816	−0.030 204 9	0.000 396 8
16	969	−0.030 207 9	0.000 401 8
17	1140	−0.030 201 0	0.000 402 7

TABLE V. Convergence behavior for the $^1D^o(1)$ state below the $N=5$ Ps threshold ($\gamma_1=\delta_1=0.2$ and $\theta=0.25$).

ω	M	E (Ry)	$\Gamma/2$ (Ry)
13	560	−0.024 671 67	2.348×10^{-5}
14	680	−0.024 672 12	2.302×10^{-5}
15	816	−0.024 672 14	2.300×10^{-5}
16	969	−0.024 672 15	2.306×10^{-5}
17	1140	−0.024 672 11	2.303×10^{-5}
18	1330	−0.024 672 14	2.302×10^{-5}

TABLE VI. Convergence behavior for the $^1D^o(2)$ state below the $N=5$ Ps threshold ($\gamma_1=\delta_1=0.19$ and $\theta=0.2$).

ω	M	E (Ry)	$\Gamma/2$ (Ry)
15	816	−0.021 915 09	2.258×10^{-5}
16	969	−0.021 914 75	2.232×10^{-5}
17	1140	−0.021 914 64	2.225×10^{-5}
18	1330	−0.021 914 58	2.235×10^{-5}

TABLE VII. Convergence behavior for the $^1D^o(3)$ state below the $N=5$ Ps threshold ($\gamma_1=\delta_1=0.2$ and $\theta=0.25$).

ω	M	E (Ry)	$\Gamma/2$ (Ry)
13	560	−0.021 358 35	0.000 114 56
14	680	−0.021 357 99	0.000 115 14
15	816	−0.021 358 11	0.000 115 00
16	969	−0.021 358 15	0.000 115 02
17	1140	−0.021 358 18	0.000 114 98
18	1330	−0.021 358 16	0.000 115 01

TABLE VIII. Resonance parameters for the $N=3$ $^3D^o(1)$ state as expansion length changes ($\gamma_1=\delta_1=0.2$ and $\theta=0.25$).

ω	M	E (Ry)	$\Gamma/2$ (Ry)
14	680	−0.055 893 58	6.39×10^{-6}
15	816	−0.055 896 53	4.72×10^{-6}
16	969	−0.055 897 36	3.01×10^{-6}
17	1140	−0.055 897 90	2.19×10^{-6}
18	1330	−0.055 898 08	1.56×10^{-6}

TABLE IX. Convergence behavior for the $^3D^o$ shape resonance lying above the $N=3$ Ps threshold with threshold energy of $-0.055\,555$ Ry ($\gamma_1=\delta_1=0.32$ and $\theta=0.6$).

ω	M	E (Ry)	$\Gamma/2$ (Ry)
12	455	−0.054 952 5	3.097×10^{-4}
13	560	−0.054 965 1	3.050×10^{-4}
14	680	−0.054 968 4	3.026×10^{-4}
15	816	−0.054 970 2	3.047×10^{-4}
16	969	−0.054 971 8	3.078×10^{-4}
17	1140	−0.054 972 2	3.106×10^{-4}

TABLE X. Convergence behavior for the $^3D^o(1)$ state below the $N=4$ Ps threshold ($\gamma_1=\delta_1=0.26$ and $\theta=0.3$).

ω	M	E (Ry)	$\Gamma/2$ (Ry)
13	560	−0.034 501 223	$1.805\,78\times10^{-4}$
14	680	−0.034 501 258	$1.805\,71\times10^{-4}$
15	816	−0.034 501 271	$1.805\,53\times10^{-4}$
16	969	−0.034 501 273	$1.805\,47\times10^{-4}$
17	1140	−0.034 501 270	$1.805\,56\times10^{-4}$

TABLE XI. Convergence behavior for the $^3D^o(2)$ state below the $N=4$ Ps threshold ($\gamma_1=\delta_1=0.2$ and $\theta=0.25$).

ω	M	E (Ry)	$\Gamma/2$ (Ry)
14	680	−0.032 696 48	1.823×10^{-6}
15	816	−0.032 695 98	1.637×10^{-6}
16	969	−0.032 695 87	1.495×10^{-6}
17	1140	−0.032 695 81	1.496×10^{-6}
18	1330	−0.032 695 79	1.501×10^{-6}

TABLE XII. Convergence behavior for the $^3D^o(1)$ resonance state below the $N=5$ Ps threshold ($\gamma_1=\delta_1=0.2$ and $\theta=0.25$).

ω	M	E (Ry)	$\Gamma/2$ (Ry)
14	680	−0.023 408 080	5.3771×10^{-5}
15	816	−0.023 408 318	5.3746×10^{-5}
16	969	−0.023 408 210	5.3803×10^{-5}
17	1140	−0.023 408 255	5.3786×10^{-5}
18	1330	−0.023 408 248	5.3777×10^{-5}

TABLE XIII. Convergence behavior for the $^3D^o$ shape resonance lying above the $N=5$ Ps threshold with threshold energy of -0.02 Ry ($\gamma_1=\delta_1=0.2$ and $\theta=0.45$).

ω	M	E (Ry)	$\Gamma/2$ (Ry)
13	560	−0.019 806 06	9.819×10^{-5}
14	680	−0.019 792 19	4.317×10^{-5}
15	816	−0.019 776 56	4.274×10^{-5}
16	969	−0.019 775 22	4.368×10^{-5}
17	1140	−0.019 776 80	4.309×10^{-5}
18	1330	−0.019 776 81	4.123×10^{-5}

Tables V–VII show the convergence behaviors for $^1D^o$ states below the $N=5$ Ps threshold (threshold energy of -0.02 Ry). Resonance parameters for the lowest three resonances $^1D^o(1)$, $^1D^o(2)$, and $^1D^o(3)$ are

$$E_r = -0.024\,672\,14 \pm 0.000\,000\,10 \text{ Ry},$$

$$\Gamma/2 = 0.000\,023\,02 \pm 0.000\,000\,10 \text{ Ry};$$

$$E_r = -0.021\,914\,58 \pm 0.000\,000\,10 \text{ Ry},$$

$$\Gamma/2 = 0.000\,022\,35 \pm 0.000\,000\,10 \text{ Ry};$$

$$E_r = -0.021\,358\,16 \pm 0.000\,000\,10 \text{ Ry},$$

$$\Gamma/2 = 0.000\,115\,01 \pm 0.000\,000\,10 \text{ Ry},$$

respectively. We will summarize all our $^1D^o$ results later in the text.

We now turn to the discussion for the $^3D^o$ results. Table VIII shows the results for the $^3D^o(1)$ state lying below the $N=3$ Ps threshold. It is seen that the resonance parameters converge extremely slowly in this case. This state is probably dominated by (df) configurations. The use of Eq. (1) with the explicit (pd) factors may lead to slow convergence. [The (df) configurations are included implicitly due to the use of various powers of r_{12} terms.] We deduce the resonance position as $E_r = -0.055\,898 \pm 0.000\,001$ Ry. As for the width, since it converges so slowly, we could only conclude that $\Gamma/2$ would be less than that obtained by using $M=1330$ terms, i.e., $\Gamma/2 < 0.000\,001\,5$ Ry. In addition to the $N=3$ Feshbach resonance, we have identified a stabilized complex eigenvalue lying above the $N=3$ threshold. We determine from Table IX the resonance parameters as $E_r = -0.054\,97 \pm 0.000\,01$ Ry and $\Gamma/2 = 0.000\,31 \pm 0.000\,01$ Ry. This shape resonance is the "symmetric" partner of the recently calculated $^1D^e$ shape resonance [6]. We will discuss the physical interpretation of these results later in the text. For the $N=4$ $^3D^o$ resonances, we have calculated resonance parameters for the lowest two

TABLE XIV. Doubly excited $^{1,3}D^o$ states of Ps^- below the Nth threshold of the Ps atom. An asterisk denotes shape resonance.

State	E_r (Ry)	$\Gamma/2$ (Ry)
	$N=3$ (threshold energy $-0.055\,555$ Ry)	
$^1D^o(1)$	$-0.060\,882\,527\,7$	$0.000\,071\,953\,7$
	$\pm 0.000\,000\,000\,2$	$0.000\,000\,000\,2$
$^3D^o(1)$	$-0.055\,898$	$< 1.5\times10^{-6}$
	$\pm 0.000\,001$	
$^3D^o(s)$*	$-0.054\,97$	$0.000\,31$
	$\pm 0.000\,01$	$\pm 0.000\,01$
	$N=4$ (threshold energy $-0.031\,25$ Ry)	
$^1D^o(1)$	$-0.037\,098\,862$	$0.000\,023\,913$
	$\pm 0.000\,000\,005$	$\pm 0.000\,000\,005$
$^1D^o(2)$	$-0.032\,722\,544$	$0.000\,013\,047$
	$\pm 0.000\,000\,010$	$\pm 0.000\,000\,010$
$^1D^o(s)$*	$-0.030\,20$	$0.000\,40$
	$\pm 0.000\,02$	$\pm 0.000\,02$
$^3D^o(1)$	$-0.034\,501\,27$	$0.000\,180\,556$
	$\pm 0.000\,000\,01$	$\pm 0.000\,000\,010$
$^3D^o(2)$	$-0.032\,695\,8$	1.50×10^{-6}
	$\pm 0.000\,000\,1$	$\pm 0.1\times10^{-6}$
	$N=5$ (threshold energy -0.02 Ry)	
$^1D^o(1)$	$-0.024\,672\,14$	$0.000\,023\,02$
	$\pm 0.000\,000\,10$	$\pm 0.000\,000\,10$
$^1D^o(2)$	$-0.021\,914\,58$	$0.000\,022\,35$
	$\pm 0.000\,000\,10$	$\pm 0.000\,000\,10$
$^1D^o(3)$	$-0.021\,358\,16$	$0.000\,115\,01$
	$\pm 0.000\,000\,10$	$\pm 0.000\,000\,10$
$^3D^o(1)$	$-0.023\,408\,25$	$0.000\,053\,78$
	$\pm 0.000\,000\,02$	$\pm 0.000\,000\,02$
$^3D^o(2)$	$-0.021\,685\,4$	1.0×10^{-6}
	$\pm 0.000\,000\,5$	$\pm 0.5\times10^{-6}$
$^3D^o(3)$	$-0.020\,975\,5$	2.77×10^{-5}
	$\pm 0.000\,001\,0$	$\pm 0.1\times10^{-5}$
$^3D^o(s)$*	$-0.019\,777$	4.1×10^{-5}
	$\pm 0.000\,003$	$\pm 0.3\times10^{-5}$

TABLE XV. Doubly excited intrashell states of Ps^- associated with the $N=3$ Ps threshold (threshold energy $-0.055\,555$ Ry).

State	$KTNn$	E_r (Ry)	$\frac{1}{2}\Gamma$ (Ry)	Resonance	Reference
$^1S^e$	2033	$-0.070\,683\,770\,8$	7.4657×10^{-5}	Feshbach	[3]
$^3P^o$	2033	$-0.069\,742\,8$	6.06×10^{-5}	Fechbach	[4]
$^1D^e$	2033	$-0.067\,828\,9$	2.56×10^{-5}	Feshbach	[6]
$^1S^e$	0033	$-0.055\,45$	$0.000\,042$	Shape	[3]
$^3P^o$	0033	$-0.054\,50$	$0.000\,46$	Shape	[7]
$^1D^e$	0033	$-0.052\,36$	$0.002\,03$	Shape	[6]
$^1P^o$	1133	$-0.063\,244\,7$	$0.000\,220\,6$	Feshbach	[4]
$^3D^e$	1133	$-0.060\,822\,5$	$0.000\,132\,2$	Feshbach	[6]
$^3P^e$	1133	$-0.063\,261\,3$	$0.000\,179\,1$	Feshbach	[5]
$^1D^o$	1133	$-0.060\,882\,527\,7$	$7.195\,37\times10^{-5}$	Feshbach	present work
$^1D^e$	0233	$-0.054\,8$	$0.000\,32$	Shape	[6]
$^3D^o$	0233	$-0.054\,97$	$0.000\,31$	Shape	present work

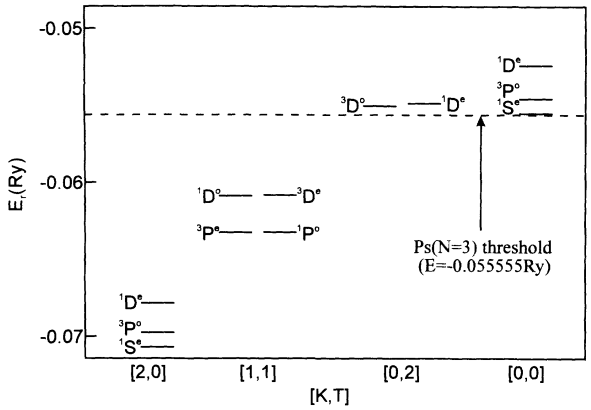

FIG. 1. Doubly excited states of Ps^- associated with the $N=3$ Ps threshold as plotted according to different rotor series.

members. From Table X the $^3D^o(1)$ is determined as $E_r=-0.034\,501\,27\pm0.000\,000\,01$ Ry and $\Gamma/2=0.000\,180\,556\pm0.000\,000\,010$ Ry. From Table XI $^3D^o(2)$ is deduced as $E_r=-0.032\,695\,8\pm0.000\,000\,1$ Ry and $\Gamma/2=1.5\times10^{-6}\pm0.1\times10^{-6}$ Ry. Results for the $N=5$ $^3D^o(1)$ state are shown in Table XII. These lead to resonance parameters of $E_r=-0.023\,408\,25\pm0.000\,000\,02$ Ry and $0.000\,053\,78\pm0.000\,000\,02$ Ry. We also calculate two more Feshbach resonances lying below the $N=5$ threshold. [Results for the $^3D^o(2)$ and $^3D^o(3)$ states are shown in Table XIV later in the text.] For the $N=5$ $^3D^o$ resonances, we have also identified a shape resonance lying above the threshold. From the results shown in Table XIII we obtain resonance parameters as $E_r=-0.019\,777\pm0.000\,003$ Ry and $\Gamma/2=4.1\times10^{-5}\pm0.3\times10^{-5}$ Ry. We summarize all our present results in Table XIV. In summary, one $^3D^o$ shape resonance each is found lying above the $N=3$ and $N=5$ Ps thresholds, respectively, and one $^1D^o$ shape resonance above the $N=4$ threshold.

IV. DISCUSSION

We now discuss a possible physical interpretation of the available doubly excited states in Ps^-. It is conjectured that the doubly excited $(e^-e^+e^-)$ three-body system behaves very much like a triatomic X-Y-X molecule. Let us look at the $N=3$ doubly excited intrashell (both electrons occupy the same shell) states in detail. Due to the vibrational character of the "molecule," the $^3P^e$ and $^1P^o$ states that have the same "quantum numbers" would be nearly degenerate. Similarly, there exist the nearly degenerate $^1D^o$ and $^3D^e$ pair as well as the $^3D^o$ and $^1D^e$ pair. We list all the available $N=3$ doubly excited intrashell states in Table XV. They are also plotted in Fig. 1. In Table XV and Fig. 1 each state is denoted by a set of quantum numbers K and T [21]. It should, however, be mentioned that in the present calculation we have not projected the K and T quantum numbers out of the wave functions. The KT assignments are simply conjectures. It is hoped that our studies would stimulate other investigations of such interesting phenomenon.

In Table XV and Fig. 1, states with the same quantum numbers are grouped together. Each group belongs to a different rotor series. The angular momentum states in each series are governed by the relationship

$$L=T,T+1,\ldots,K+N-1\ . \tag{11}$$

For example, for the series with quantum numbers ($K=2$ and $T=0$), the rotor starts with $L=0$ and ends at $L=4$ (for $N=3$). So far only the $^1S^e$, $^3P^o$, and $^1D^e$ states for the series have been calculated. It would be of great interest to investigate $^3F^o$ and $^1G^e$ resonances. For $K=0$, $T=0$, and $N=3$, the series starts from a $^1S^e$ and ends with a $^1D^e$ states. From the numerical calculations, all these three members ($^1S^e$, $^3P^o$, and $^1D^e$) are found lying above the threshold and become shape resonances. As for the $K=0$, $T=2$, and $N=3$ series, only D-wave states are allowed [see Eq. (11)]. Our calculations indicate that both the $^3D^o$ and $^1D^e$ states are shape resonances.

In summary, we have presented a complex-coordinate rotation calculation for doubly excited $^1D^o$ and $^3D^o$ states of Ps^- associated with the $N=3$, 4, and 5 Ps thresholds. Feshbach and shape resonances are examined. Our results, obtained by using elaborate Hylleraas functions, are useful references for future theoretical and experimental studies of this three-particle system.

ACKNOWLEDGMENTS

Y.K.H is supported by the National Science Council under Grant No. NSC 83-0208-M-001-105.

[1] Y. K. Ho, Phys. Rep. **99**, 1 (1983).
[2] Y. K. Ho, Phys. Rev. A **19**, 2347 (1979); Phys. Lett. **102A**, 348 (1984) and (unpublished).
[3] Y. K. Ho, Hyperfine Interac. (to be published).
[4] A. K. Bhatia and Y. K. Ho, Phys. Rev. A **42**, 1119 (1990); Y. K. Ho and A. K. Bhatia, *ibid.* **44**, 2890 (1991).
[5] Y. K. Ho and A. K. Bhatia, Phys. Rev. A **45**, 6268 (1992).
[6] A. K. Bhatia and Y. K. Ho, Phys. Rev. A **48**, 264 (1993).
[7] Y. K. Ho and A. K. Bhatia, Phys. Rev. A **47**, 1497 (1993).
[8] A. P. Mills, Jr., Phys. Rev. Lett. **46**, 717 (1981).
[9] A. P. Mills, Jr., Phys. Rev. Lett. **50**, 671 (1983); A. P. Mills, Jr., in *Annihilation in Gases and Galaxies,* edited by R. J. Drachman, NASA Conf. Publ. 3058 (NASA, Washington, DC, 1990), p. 213.
[10] Y. K. Ho, J. Phys. B **16**, 1503 (1983); Phys. Lett. A **144**, 237 (1990); Phys. Rev. A **48**, 4780 (1993).
[11] A. K. Bhatia and R. J. Drachman, Phys. Rev. A **28**, 2523 (1983).
[12] A. M. Frolov, J. Phys. B **26**, 1031 (1993); A. M. Frolov and A. Y. Yeremin, *ibid.* **22**, 1263 (1989); A. M. Frolov and D. M. Bishop, Phys. Rev. A **45**, 6236 (1992).
[13] P. Petelenz and V. H. Smith, Jr., Phys. Rev. A **36**, 5125 (1987).
[14] M. I. Haftel and V. B. Mandelzweig, Phys. Rev. A **39**, 2813 (1989); R. Krivec, M. I. Haftel, and V. B. Mandelzweig, *ibid.* **47**, 911 (1993).

[15] G. W. F. Drake (unpublished).
[16] D. M. Schrader, in *Positron Annihilation,* edited by P. G. Coleman, S. C. Sharma, and L. M. Diana (North-Holland, Amsterdam, 1982), p. 71.
[17] Y. K. Ho, in *Annihilation in Gases and Galaxies* (Ref. [9]), p. 243.
[18] Y. K. Ho, Hyperfine Interact. **73**, 109 (1992).
[19] A. K. Bhatia, Phys. Rev. A **6**, 2498 (1972).
[20] A. K. Bhatia and A. Temkin, Rev. Mod. Phys. **36**, 1050 (1964).
[21] D. R. Herrick, Adv. Chem. Phys. **52**, 1 (1983); C. D. Lin, Adv. At. Mol. Phys. **22**, 77 (1986).